ChemPubSoc Europe

DOI: 10.1002/slct.201904010

Chemistry SELECT Full Papers

Catalysis

Metal-Ceramic Composites for Photocatalytic Oxidation of Diclofenac in Aqueous Solution

Maria V. Sherstoboeva,[a] Anastasiya V. Bavykina,*[b] Konstantin A. Bolgaru,[c] Yury M. Maksimov,[c] Francesc Sastre,[d] and Lidia N. Skvortsova[a]

Photocatalytic activity of metal-ceramic composites synthesized by self-propagating high-temperature synthesis (SHS) is investigated in the processes of degradation of diclofenac (DCF). Optical properties of the composites were studied, and the band gaps of ceramic matrix semiconducting components were calculated from the absorbance spectra. The effect of the phase composition, UV irradiation duration, the nature and quantity of the activator ($H_2C_2O_4$ and H_2O_2) on the degree of oxidation destruction was investigated. The best catalytic performance (98–99% DCF degradation) was achieved with the combination of heterogeneous boron nitride and SiAlON based composites and a homogeneous photo-Fenton system. However, DCF decomposition with a minimum number of intermediates was achieved using boron nitride-based composites.

1. Introduction

Water pollution problem has been jeopardizing our health for decades. Water is being contaminated with pharmaceutical drugs and their metabolites, coming from wastewater. These wastes -so-called organic micropollutants (OMP)- are highly toxic even when present at ppb levels.[1] Currently, industrial practices predominantly utilize Advanced Oxidation Processes (AOP) to remove pharmaceutical residues from aqueous flows. AOP involve highly reactive hydroxyl radicals formation. These radicals are effective in oxidative degradation of a wide range of organic pollutants under mild conditions,[2,3] which can be used for either pre- or post- water treatment. The pretreatment comprises partial oxidation into more biodegradable product (HCOOH, CH_2O *etc*..) that can be further destroyed by traditional biological treatment using microorganisms. The post-treatment is traditionally preferred; it follows up traditional destruction methods that include ozonation to decompose OMP into CO_2, H_2O and inorganic ions. The use of an easily recoverable and cheap heterogeneous catalyst would undeniably be beneficial for this process.

Iron-based catalysts are of particular interest from the economic and environmental points of view. The photo-Fenton system is one of the most efficient Fe based homogeneous systems for AOP. It comprises $Fe^{3+}/Fe^{2+} + H_2O_2$ combined with ultraviolet light, a cyclic reaction which is highly effective as a renewable source of the hydroxyl radicals.[4–6] However, for the photo-Fenton system, pH range should be low (2–3) in order to prevent Fe ions hydrolysis. This issue can be overcome by the use of ferrioxalic system –a soluble iron complex dissolved in a weak acidic or neutral solution.[7,8] Moreover, ferrioxalic system makes it possible to use softer UV radiation, since ferrioxalate complex $[Fe(C_2O_4)_3]^{3-}$ absorbs in the near UV radiation at 350 nm in contrast to the photo-Fenton system that has an absorption band at 250 nm at pH 1.5. In one of the most recent reports, the authors have shown that incorporation of Fe(III) complex (Fe(III) tetra(*4*-carboxylphenyl)porphyrin chloride (Fe^{III}-TCPPCl) within the pore of zirconium based metal organic framework (UiO-66 MOF) enhanced degradation of organic contaminants under visible light irradiation.[9] There, the acceleration of the Fenton-like reaction under visible light irradiation has been achieved with the help of mixed ligand Fe^{III}-TCPPCl, that not only played the role of a photosensitizer but also suppressed the recombination of photo-induced carriers over the integrated structure.

Previous research has shown that iron-ceramic composites based on boron nitrides and silicon nitrides had high photocatalytic activity in the processes of degradation of phenolic compounds -formaldehyde, oxalic acid and some dyes- due to the formation of photoactive catalytic systems (photo-Fenton and ferrioxalic) in the presence of activators (H_2O_2 and $H_2C_2O_4$).[10,11] Moreover, when utilizing this composites, dissolved iron concentration in a solution does not exceed 10^{-3} mg L^{-1}, so there is no need in the additional step of iron removal from thereafter.

[a] *M. V. Sherstoboeva, Dr. L. N. Skvortsova*
Chemical Faculty/Analytical Chemistry Department
National Research Tomsk State University
36 Lenin Ave., Tomsk, 634050 (Russia)
[b] *Dr. A. V. Bavykina*
KAUST Catalysis Center (KCC), Advanced Catalytic Materials
King Abdullah University of Science and Technology
Thuwal 23955-6900 (Saudi Arabia)
E-mail: anastasiya.bavykina@kaust.edu.sa
[c] *Dr. K. A. Bolgaru, Prof. Y. M. Maksimov*
Department of Structural Macrokinetics
Tomsk Scientific Center of the Siberian Branch of the Russian Academy of Sciences (SBRAS)
10/3 Academichesky Ave., Tomsk 634021 (Russia)
[d] *Dr. F. Sastre*
The Netherlands Organization for Applied Scientific Research (TNO)
High Tech Campus 25, 5656AE Eindhoven, The Netherlands

Supporting information for this article is available on the WWW under https://doi.org/10.1002/slct.201904010

Diclorofenac (DCF) is included in the List of life-saving and essential medicinal products. However, according to the European Environmental Agency, DCF is also being a prevalent water pollutant.[12] During the last years, the concern about DCF removal from aqueous media by different methods has increased considerably.[13–15] The research of various Fe-containing catalysts for DCF degradation under catalytic ozonation showed that the though mineralization rate achieved *ca.* 75%, the formed intermediates are more toxic than DCF itself.[16,17] High oxidation destruction of DCF with 84% rate was shown with a heterogeneous photo-Fenton-like process with $FeCeO_x$ catalyst.[18] An immobilized TiO_2-based zeolite composite (TiO_2-FeZ) also showed high efficiency in removal of DCF by water treatment with an addition of H_2O_2 for photo-Fenton system creation under simulated solar irradiation due to good DCF adsorption on the catalyst.[19]

Herein, we further explore the advantages possessed by metal-ceramic composites in the photocatalytic degradation of organic pollutants and pharmaceutical residues, including DCF. The composite materials based on nitrides of boron, silicon, chromium, and SiAlON were synthesized by self-propagating high-temperature synthesis (SHS) technology according to previous developed techniques.[20] SHS method involves a formation of combustion products as the result of exothermic reactions under burning-wave propagation towards "cold" layers of the reagents due to heat evolution. Burning wave derives from the local reaction initiation by a heat pulse of an external power supply. The SHS method is one of the most cost-effective methods for nitrides production due to low energy cost, which also allows easy handling and single-step synthesis process. To reduce the cost of photocatalysts and for environmental reasons, wastes from ferroalloy industry (Yurginsky Abrasive Plant, Russia) were used for composite synthesis instead of commercial highly dispersed powders of boron, chromium and oxides of silicon and aluminum.

The parameters affecting the degree of DCF oxidation destruction such as the phase composition of the catalysts, addition of $H_2C_2O_4$ and H_2O_2 are investigated and the optimal conditions for the most effective photocatalysis have been proposed.

2. Results and Discussion

2.1. Characterization of the Composites

The phase composition of the composites, obtained by the means of X-ray diffraction (XRD), is given in Table 1. XRD patterns of the composites are given in Supporting Information (SI) (Figure S1). Ceramic matrices of the composites are based on the wide-bandgap semiconductors BN, Si_3N_4, $Si_3Al_3O_3N_5$ and CrN. The BN composite was obtained by nitriding of ferroboron with an additive of urea as a pore-forming agent. The SiN composite was obtained by nitriding of ferrosilicon. The SiAlON and TiN composites are the products of ferrosilicon-aluminum (FSA) pyrolysis. For the TiN composite metal titanium was added. Surface morphology of the materials was investigated by scanning electron microscopy (SEM) and energy-dispersive X-ray spectroscopy (Figure S2).

Table 1.

Composite	Phase composition	Calculated E_g, eV	Main semiconducting phase	Reference E_g, eV
BN	**α-BN**,[a] α-Fe, $FeB + Fe_2B$	5.3	α-BN	4.0-5.8 [22]
SiN	**β-Si_3N_4**, α-Fe, Fe_xSi_y	2.3	β-Si_3N_4	4.0-4.5[23]
SiAlON	**β-$Si_3Al_3O_3N_5$**, α-Fe	4.3	$Si_{6-x}Al_xO_xN_{8-x}$	2.3-5.3 [25]
TiN	**TiN**, β-Si_3N_4, α-Si_3N_4, Fe, Fe_xSi_y	3.2	TiN	3.4[21]
CrN	**CrN**, Cr_2N	0.1	CrN	0.07-0.09[26]

[a] The main phase of a composite is in **bold.**

2.2. Optical Properties of the Composites

Optical properties of the composites were studied by means of the electronic absorption spectrometry (Figure 1). The spectra show that BN composite displays the lowest absorption. The absorption peak at 250 nm is attributed to the absorption of unreacted ferroboron (Figure S3). The SiN and SiAlON composites have the absorption peaks in the UV range of 200–300 nm, which can be attributed to the main phases of SiN and SiAlON, respectively. Higher absorption efficiency in the UV and visible range of 250–800 nm is demonstrated by the composites based on titanium and chromium nitrides. The higher absorption efficiency of the composite containing titanium nitride phase in visible spectrum can be explained by the formation of Ti-N bond .[21]

The absorption coefficient dependences on the photon energy for the composites are shown in Figure 2. Semiconductors CrN and Si_3N_4 in the composites of CrN and SiN have indirect badgaps. There the energy change upon light

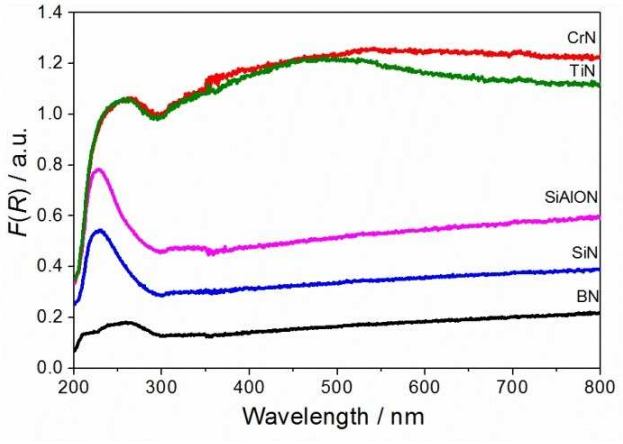

Figure 1. Absorption spectra of iron-ceramic composites.

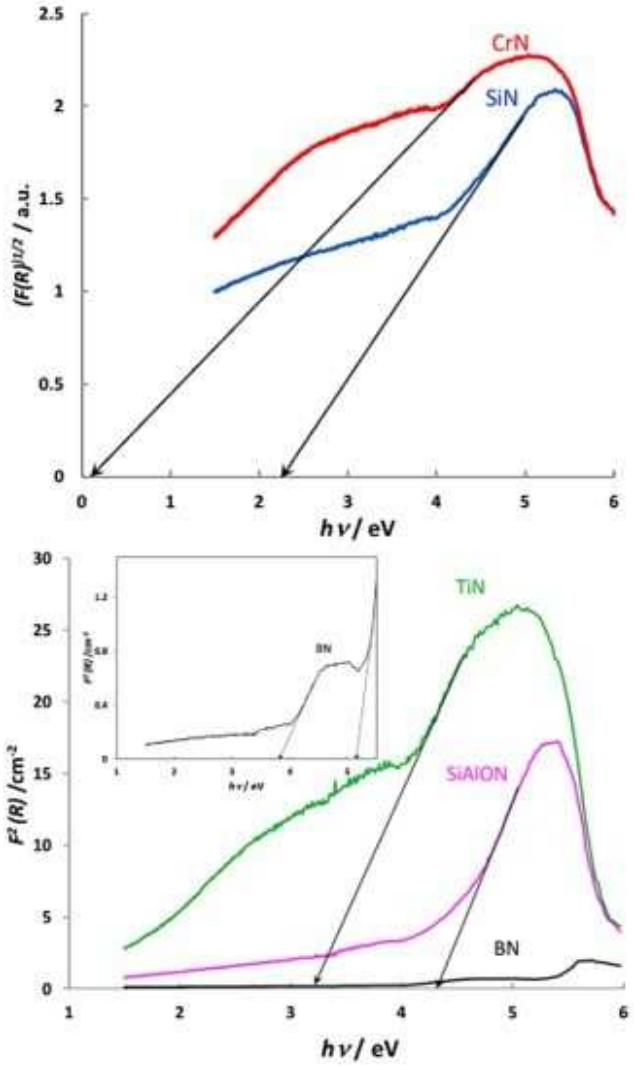

Figure 2. Dependence of absorption coefficient on photon energy for the composites with (A) indirect and (B) direct electronic transitions.

photon absorbtion by electron is accompanied by the energy change of the crystal lattice. For the indirect electronic transitions, the dependence of the absorption coefficient versus photon energy is described $F(R)^{1/2}=f(h\nu)$ (Figure 2A). In semiconductors BN, TiN and $Si_3Al_3O_3N_5$, only photon and electron participate in electronic transitions from valence band to transition band when absorbing light photon; so they have direct bandgap. The absorption edge and bandgap energy of these semiconductors were determined using $F(R)^2=f(h\nu)$ dependence (Figure 2B).

Table 1 presents calculated optical band gap (E_g) values of the studied composites, which are in the line with the literature data of the ceramic matrix constituent phases.

According to X-ray diffraction analysis and electronic microscopy, boron nitride has α-modification with hexagonal crystalline structure (Figure S1A). The band gap values fluctuation for α-BN comes from the different synthesis methods of the composite.[22] SiN composite has a narrower band gap than bulk silicon nitride, which is likely due to the presence of the narrow band gap iron silicide Fe_xSi_y ($E_g \sim 0{,}9$ eV) in the matrix.[23] The valence band of silicon nitride consists of two sub-bands.[24] It seems likely that iron silicide facilitates interband transitions and enhances conductivity.

SiAlON is a solid solution of variable composition $Si_{6-x}Al_xO_xN_{8-x}$ that is formed by the substitution of Si to Al and of N to O in β-silicon nitride. The band gap of SiAlON is strongly dependent on stoichiometry.[23] TiN composite has an absorption edge corresponding to the band gap $E_g = 3.2$ eV referring to *n*-type TiN. Chromium nitride-based composite mainly consists of two-dimensional CrN that can display the properties of narrow band gap semiconductor.[24] To sum up, the band gap of the semiconductors incorporated in a ceramic matrix of the composites used in the study is lower than the photon energy of irradiated light (4.5–5.0 eV) suggesting the possibility of the composites to be active as photocalysts.

2.3. Acid-base Surface Sites of the Composites

The composite surface active sites were investigated using Hammett indicators following Tanabe method with spectrophotometric indication according to the technique described.[27] Figure 3 shows curves of distribution of surface acid-base sites with a certain pK_a value. It can be seen that the surfaces of BN, SiN and SiAlON composites were predominated by the aprotic Lewis base sites and strong Brønsted acid sites. The weak Brønsted acid sites predominated on the TiN composite surface. The smallest amount of surface sites was on the CrN-based composite.

The distribution of surface active sites was also determined for the phases of ferroboron, boron nitride, metallic (carbonyl) iron and Al_2O_3 (Figure S4).

It can be seen that the Lewis base sites and the Brønsted protolytic sites were formed by two phases – ferroboron and boron nitride. The strong Brønsted acid sites with pK_a 0–7 are formed as a result of complete or partial hydration of iron, aluminium, boron and silicon, and the weak Brønsted acid sites

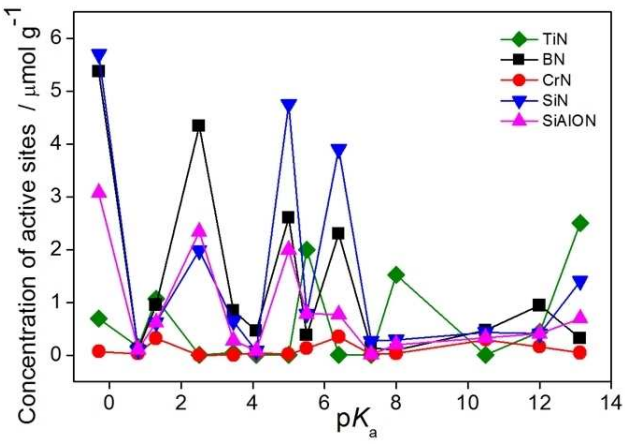

Figure 3. Distribution of adsorption sites of the dye indicators on the composite surface.

(pK_a 7–14) as a result of the hydration of the Lewis aprotic sites. Metallic iron forms on its surface a weak acid site with pK_a 6.4. The surface active sites of the composites are shown in Table S2 and the functions of the surface acidity of the composites are shown in Table 2.

The values obtained confirm the weakly acid nature of the materials except for the TiN-based composite.

Thus, variety of the Lewis and Brønsted sites on the surface of the composites suggests their high adsorption capacity to a wide range of organic compounds.

2.4. Photocatalytic Activity of the Composites

Despite the fact that the composite can absorb in the visible zone, UV irradiation was used in order to generate the classic photo-Fenton system. The photocatalytic activity of the composites in the process of DCF degradation (Table 3) have shown the DCF adsorption by BN, SiN and SiAlON composites is 10–15% higher than that of the TiN and CrN ones. This may be explained by the increase of the number of strong Brønsted acid sites (FeOH-$H^{\delta+}$, BO-$H^{\delta+}$, SiO-$H^{\delta+}$) with $pK_a = 4.10$ from 0.2 to 0.4 μmol g^{-1} on their surfaces.[25] Thus, the correlation between the degree of DCF adsorption by the composites and degree of DCF UV photodegradation is present.

The following mechanism of DCF adsorption has been proposed taking into account the nature of active surface sites of metal-ceramic composites (Eqs. (1-4)):

$$/SiO\text{-}H^{\delta+} + C_{14}H_{10}Cl_2NO_2^- \rightarrow /SiO\text{-}H\ldots C_{14}H_{10}Cl_2NO_2 \quad (1)$$

$$/BO\text{-}H^{\delta+} + C_{14}H_{10}Cl_2NO_2^- \rightarrow /BO\text{-}H\ldots C_{14}H_{10}Cl_2NO_2 \quad (2)$$

$$/FeOH\text{-}H^{\delta+} + C_{14}H_{10}Cl_2NO_2^- \rightarrow /FeOH\text{-}H\ldots C_{14}H_{10}C_{l2}NO_2 \quad (3)$$

$$/AlOH\text{-}H^{\delta+} + C_{14}H_{10}Cl_2NO_2^- \rightarrow /AlOH\text{-}H\ldots C_{14}H_{10}C_{l2}NO_2 \quad (4)$$

Table 2. Optical properties of the composites and constituent semiconducting phases.

Composite	BN	SiN	SiAlON	TiN	CrN
H0	4.2	4.3	3.4	7.8	4.7

Table 3. Adsorption degree (%) and the degree of DCF photodegradation (%) over metal-ceramic composites under different conditions (DCF concentration is 25 mg l^{-1}, $H_2C_2O_4$ concentration is $5\cdot10^{-5}$ M, H_2O_2 concentration is $1\cdot10^{-4}$ M, catalyst weight is 100 mg, solution volume is 10 ml, UV irradiation duration is 30 min).

Composite	ω(Fe), %	Adsorption	UV	UV/$H_2C_2O_4$	UV/$H_2C_2O_4$/H_2O_2
No composite	–	6	31	32	34
BN	5–35	36	89	91	89
SiN	4–34	31	60	69	65
SiAlON	1.6–2.5	32	58	61	72
TiN	2.0–4.7	19	59	60	76
CrN	–	17	43	69	77

Thus, the correlation between the degree of DCF adsorption by the composites and degree of DCF UV photodegradation is present.

In order to enhance the DCF degradation using *in-situ* formed homogeneous catalyst, $H_2C_2O_4$ and $H_2C_2O_4/H_2O_2$ were added to the solution along the composite. There. the partially dissolved metal iron phase offers the right conditions for the ferrioxalic system and photo-Fenton process to generate ·OH radicals.

It is seen from the results shown in Table 3, that the degree of DCF degradation under UV radiation with and without the addition of $H_2C_2O_4$ is similar within the experimental errors for all the composites. This indicates a prevailing role of heterogeneous photocatalysis in the process DCF degradation. However, with chromium nitride-based composite and addition of $H_2C_2O_4$, the degree of DCF degradation increased up to 25%, suggesting homogeneous catalysis. A possible explanation is that a photoactive complex $[Cr(C_2O_4)_3]^{3-}$ generating ·OH radicals (Eqs. (5–10)), similar to ferrioxalate complex $[Fe(C_2O_4)_3]^{3-}$, is being formed in a solution in the presence of $H_2C_2O_4$.[28]

$$[Cr^{III}(C_2O_4)_3]^{3-} + h\nu \rightarrow [Cr^{II}(C_2O_4)_2(C_2O_4^{\bullet-})]^{3-} \quad (5)$$

$$[Cr^{II}(C_2O_4)_2(C_2O_4^{\bullet-})]^{3-} + O_2 + 2H_2O \rightarrow [Cr^{III}(C_2O_4)_2(H_2O)_2]^- + C_2O_4^{\bullet-} + O_2^{--} \quad (6)$$

$$C_2O_4^{\bullet-} \rightarrow CO_2^{\bullet-} + CO_2 \quad (7)$$

$$CO_2 + O_2^{\bullet-} \rightarrow CO_2 + O_2^{\bullet-} \quad (8)$$

$$Cr^{2+} + O_2^{\bullet-} + 2H^+ \rightarrow Cr^{3++}H_2O_2 \quad (9)$$

$$Cr^{2+} + H_2O_2 \rightarrow Cr^{3+} + {}^{\cdot}OH + OH^- \quad (10)$$

The combined peroxide/ferrioxalate system (UV/$H_2C_2O_4$/H_2O_2) resulted in a slight increase of the degree of DCF degradation in the presence of the most composites studied here that indicates a small role of a photo-Fenton process.

In order to confirm the participation of a composite matrix in photocatalysis, a hot filtration test was performed. The catalyst was removed from the reaction solution by filtration after 10 min of irradiation while the solution continued being irradiated. After 15 min, the composite was added back to the reaction solution, and the photocatalytic process was continued for 10 min more. The DCF concentration was determined every 5 min by spectrophotometry.

From the Figure 4, it is seen that the removal of the composites from a solution results in the rate reduction of the DCF oxidation degradation, and the reaction rate is increased again after placing the catalyst back within the reaction mixture. This phenomenon indicates the involvement of the composite matrix in the photocatalytic process, thus confirming the heterogeneous nature of the process. When the composite is being removed from the solution, the DCF

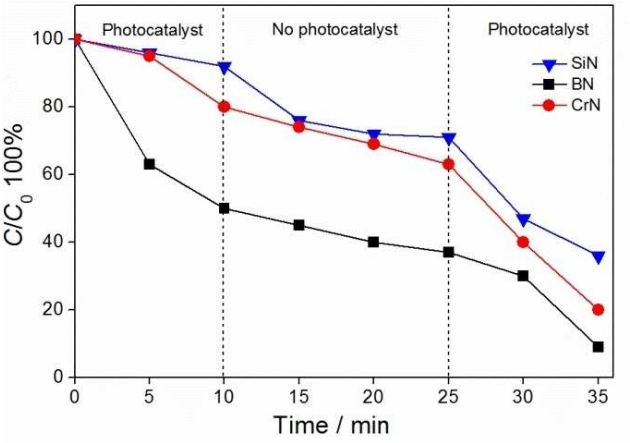

Figure 4. Dependence of the degree of DCF photocatalytic destruction on time when a composite is removed from a reaction solution (from t = 10 min until t = 25 min) during UV irradiation.

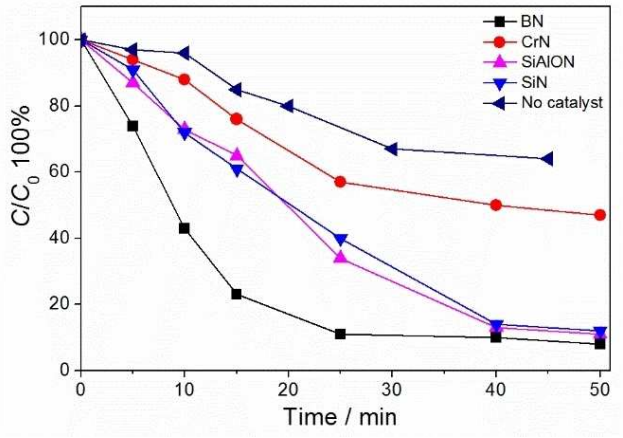

Figure 5. The effect of UV radiation duration on the degree of DCF degradation with and without the composites in a solution. Only UV light was used, no additions of H_2O_2 or $C_2H_2O_2$.

oxidation proceeds under homogeneous catalysis accompanied by the negligible dissolution of the phase of metallic iron or chromium nitride Cr_2N when initially being in contact with a solution and generation of hydroxyl radicals $^{\bullet}OH$ according to Eqs. (11–14):

$$[Fe(H_2O)]^{3+} + h\nu \rightarrow Fe^{2+} + HO^{\bullet} + H^{+} \quad (11)$$

$$[Fe(OH)]^{2+} + h\nu \rightarrow Fe^{2+} + HO^{\bullet} \quad (12)$$

$$[Fe(OOC\text{-}R)]^{2+} + h\nu \rightarrow Fe^{2+} + CO_2 + R^{\bullet} \quad (13)$$

$$[Cr(H_2O)]^{3+} + h\nu \rightarrow Cr^{2+} + HO^{\bullet} + H^{+} \quad (14)$$

As a result, the activity of metal-ceramic composites in photocatalytic DCF degradation is defined by the combination of heterogeneous and homogeneous catalysis.

The investigation of the effect of UV radiation duration on the degree of DCF degradation (Figure 5) has shown that the DCF destruction with most composites achieves ca. 90% after 40 min except for CrN composite for which it does not exceed 50%. The low degree of DCF degradation (*ca.* 35%) when there is no composite in a solution indicates high photocatalytic activity of the metal-ceramic composites.

It should be noted that the degree of DCF degradation with the boron nitride-base composite (BN composite) achieves 80% after 15 min of irradiation (Figure 5). Then, the degradation rate declines. In this regard, we studied the possibility for increasing the degree of degradation and improving energy efficiency by decreasing the exposure time down to 15 min by enhancing a role of homogeneous catalysis. For this reason, H_2O_2 was added to a reaction solution to produce the photo-Fenton system that generates hydroxyl radicals $^{\bullet}OH$. The results of the investigation of the DCF oxidation degradation with the composites and H_2O_2 addition (Table 4) have shown a considerable increase of the degree of DCF degradation when H_2O_2 is added to a solution. Moreover, a tenfold increase in H_2O_2 concentration results in the almost total degradation of DCF with the composites based on boron nitride, titanium nitride and SiAlON (BN, SiAlON and TiN composites). This confirms that the enhancement efficiency of photocatalytic DCF oxidation destruction with H_2O_2 addition is connected with the participation of hydroxyl radicals $^{\bullet}OH$ generated in a photo-Fenton reaction.

Table 4. The effect of H_2O_2 concentration on the degree of DCF degradation (%) over metal-ceramic composites under photo-Fenton conditions (DCF concentration is 25 mg l^{-1}, catalyst weight is 100 mg, solution volume is 10 ml, UV irradiation duration is 15 min).

Composite	UV, without H_2O_2	(UV + H_2O_2) c_{H2O2}, mol l^{-1}	
		$1 \cdot 10^{-4}$	$2 \cdot 10^{-3}$
BN	77	78	98
SiN	49	65	75
SiAlON	45	81	99
TiN	56	74	92
CrN	24	73	77

The possibility of decreasing the UV irradiation duration by increasing the catalyst amount was also investigated.

The results of the effect of the composite (TiN) weight on the degree of DCF degradation (Figure 6) show that increasing the catalyst weight in the range of 100 to 500 mg leads to a small increase (*ca.* 15%) in the degree of DCF degradation. Further increasing of composite added to the reaction, up to 500 mg does lead to an increase of the DCF degradation. We found an optimal point for this reaction of 300 mg of composite. Same dependences have been obtained for other composites (Table S3).

The role of adsorption of DCF by the catalysts was investigated by infrared (IR) spectroscopy. For this purpose, IR spectra of the composites were recorded before and after DCF photocatalytic degradation in the range of 400–4000 cm^{-1} on Thermo Scientific Nicolet 6700 FT-IR Spectrometer (Thermo Scientific, USA) (Figure 7).

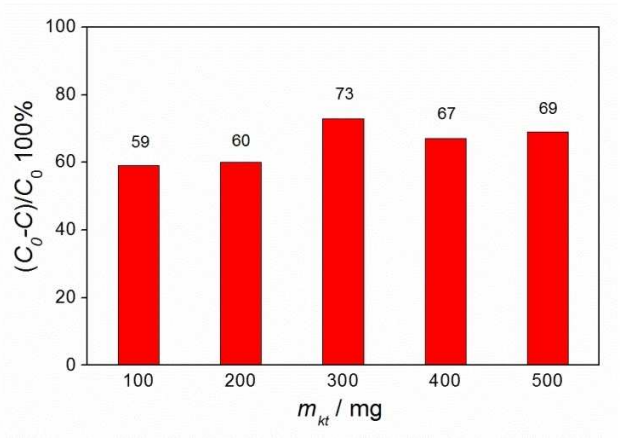

Figure 6. The effect of weight of TiN composite on the degree of DCF degradation under UV irradiation; experimental error does not exceed 7%.

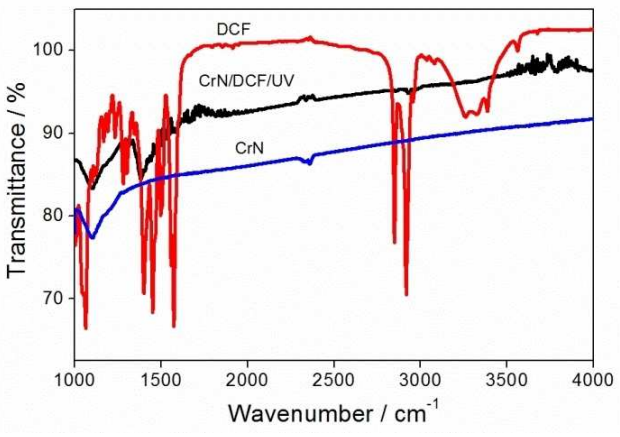

Figure 7. IR-spectra of DCF and CrN composite before and after photoctalytical degradation of DCF.

After photocatalysis, the characteristic DCF absorption peaks were weak or absent in the IR spectra of BN, SiAlON and TiN composites that may indicate the degradation of large part of DCF in a solution. After photocatalytic experiments with the silicon nitride-base composite, a shoulder emerged in the infrared range of 1100–900 cm^{-1}, which can be attributed to the aromatic C-H in-plane and out-of-plane bending vibrations from molecule DCF. In the IR spectra of CrN composite, some weak peaks emerged in the range of 1400–800 cm^{-1}, which is typical for asymmetric and symmetric vibrations of C-O group of the carboxylate ion from molecule DCF. These results confirm that DCF and its intermediates hardly adsorbed by the composites while being considerably destroyed in the reaction solution.

2.5. DCF Intermediates

In order to assess how complete the DCF photocatalytic destruction over metal-ceramic composites, the reaction solutions were analyzed by reversed phase high-performance liquid chromatography (RP-HPLC).[29--31] The DCF peak on the chromatograms has decreased more than 10 times (Figure S5), in particular in case of SiAlON and TiN composites, upon UV irradiation for 30 min of the combined heterogeneous photo-Fenton system ($c_{H2O2} = 2 \cdot 10^{-3}$ M). However, four new peaks of degradation products emerged in a chromatogram at $\lambda =$ 250 nm in the range of $\tau_R = 2$–5 min. It is obvious (Figure S5) that more complete and deep degradation of DCF achieves with a composite based on boron nitride.

2.6. Stability of the Composites

The stability was estimated of the most active composites BN and SiAlON in the process of DCF degradation. The results of catalyst testing in repetitive cycles are shown in Figure 8. The degradation rate of DCF was found to be gradually decreased after repetitive cycles. However, the catalytic activity remained at high level (more than 90%) during first three cycles. After three cycles, the DCF degradation rate was decreased more considerably for SiAlON sample. This may be connected with less Fe content in SiAlON sample in comparison to BN composite, which is being leached out of the ceramic matrix decreasing the activity of photo-Fenton process.

According to XRD analysis, the diffractograms of BN composite remained practically identical after five cycles of oxidative DCF degradation to the original one (Figure S6). A peak of metallic iron slightly decreased, and a small peak of adsorbed DCF degradation intermediate (Peak at 21 2θ, marked with an arrow) appeared on the BN diffractogram. After five repetitive catalytic experiments of SiAlON composite, a diffraction peak of metallic Fe notably decreased and the ratio of SiAlON diffraction peaks was changed (Figure S7). This may be caused by deviation in the composite stoichiometry.

3. Conclusions

Diffusion reflection spectroscopy has shown that the composites materials based on nitrides of silicon, titanium, boron and

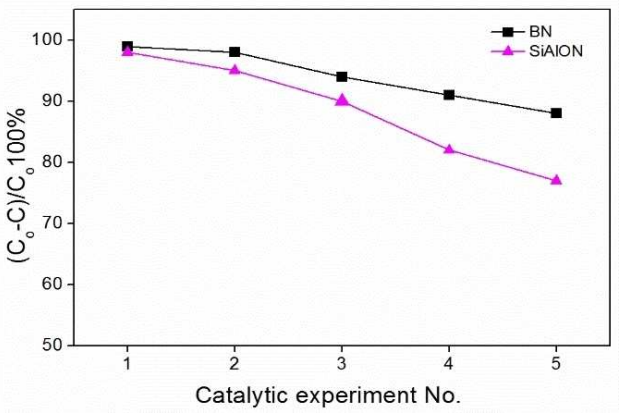

Figure 8. The rate of DCF degradation after several photocatalytic experiments.

chromium, and SiAlON can be used in heterogeneous photocatalysis for DCF degradation. This composites materials and absorb UV radiation (E_g = 0.1-5.3 eV). Moreover, iron-ceramic catalysts together with $H_2C_2O_4$ and H_2O_2 creates conditions for homogeneous catalysis with the participation of ferrioxalate [$Fe(C_2O_4)_3]^{3-}$, chromium oxalate [$Cr(C_2O_4)_3]^{3-}$ and a Fenton reagent (UV/Fe(II,III)/H_2O_2) producing hydroxyl radicals. A correlation between DCF physisorption activity of the composites and the degree of photodegradation under UV radiation has been observed. The role of heterogeneous photocatalysis under UV irradiation has been shown by the separation of a catalyst from a solution. High efficiency of DCF oxidation destruction with the iron-ceramic composites has been resulted from the combination of heterogeneous and homogeneous catalysis. The most favorable condition for DCF decomposition is the combination of heterogeneous catalysis using the composites based on boron nitride and SiAlON with good adsorption activity and the homogeneous photo-Fenton system ($c(H_2O_2) = 2 \cdot 10^{-3}$ mol l^{-1}, τ_{UV} = 15 min) that reduced the DCF in 98%.

Summary Information

The Supporting Information (SI) file presents the following information: a method of synthesis of metal-ceramic composites in more detail, an analytical technique for DCF control, description of photocatalytical experiments, XRD data for investigation of phase composition and stability of photocatalysts, and electron microscope images of composite surface. Also, SI includes a description of experimental investigation of surface acid-base sites of the composites, optical properties and RP-HPLC chromatograms for DCF photocatalytical degradation products.

Acknowledgements

This study was supported by the Tomsk State University competitiveness improvement programme. The work was carried out within the state task of The RF Ministry of Education and Science (N° 0365-2019-0005)

Keywords: diclofenac · heterogeneous photocatalysis · homogeneous photocatalysis · metal-ceramic composites · photo-Fenton

[1] A. R. Ribeiro, O. C. Nunes, M. F. R. Pereira, A. M. T. Silva, *Environ. Int.* **2015**, *75*, 33–51.
[2] Y. Deng, R. Zhao, *Curr. Pollut. Rep.* **2015**, *1*, 167–176.
[3] W. H. Glaze, J.-W. Kang, D. H. Chapin, *Ozone Sci. Eng.* **1987**, *9*, 335–352.
[4] R. Ameta, A. K. Chohadia, A. Jain, P. B. Punjabi, *Advanced Oxidation Processes for Waste Water Treatment* (Eds.: S. C. Ameta, R. Ameta), Academic Press **2018**, pp. 49–87.
[5] A. Babuponnusami, K. Muthukumar, *J. Environ. Chem. Eng.* **2014**, *2*, 557–572.
[6] N. Klamerth, S. Malato, M. I. Maldonado, A. Agüera, A. R. Fernández-Alba, *Environ. Sci. Technol.* **2010**, *44*, 1792–1798.
[7] J. M. Monteagudo, A. Durán, C. López-Almodóvar, *Appl. Catal. B* **2008**, *83*, 46–55.
[8] D. Prato-Garcia, R. Vasquez-Medrano, M. Hernandez-Esparza, *Sol. Energy* **2009**, *83*, 306–315.
[9] L. Wang, P. Jin, S. Duan, J. Huang, H. She, Q. Wang, T. An *J. Environ. Sci.: Nano* **2019**, 6, 2652–2661.
[10] L. N. Skvortsova, L. N. Chukhlomina, V. N. Batalova, *Rus. J. Appl. Chem.* **2014**, *87*, 1686–1692.
[11] L. N. Skvortsova, L. N. Chukhlomina, G. M. Mokrousov, A. E. Krotov, *Rus. J. Appl. Chem.* **2013**, *86*, 37–41.
[12] M. O. Barbosa, N. F. F. Moreira, A. R. Ribeiro, M. F. R. Pereira, A. M. T. Silva, *Water Res.* **2016**, *94*, 257–279.
[13] A. V. Hallare, H. R. Köhler, R. Triebskorn, *Chemosphere* **2004**, *56*, 659–666.
[14] M. Letzel, G. Metzner, T. Letzel, *Environ. Int.* **2009**, *35*, 363–368.
[15] L. Lonappan, S. K. Brar, R. K. Das, M. Verma, R. Y. Surampalli, *Environ. Int.* **2016**, *96*, 127–138.
[16] W. Chen, X. Li, Z. Pan, S. Ma, L. Li, *Chem. Eng. J.* **2016**, *304*, 594–601.
[17] G. Gao, J. Shen, W. Chu, Z. Chen, L. Yuan, *Sep. Purif. Technol.* **2017**, *173*, 55–62.
[18] S. Chong, G. Zhang, N. Zhang, Y. Liu, T. Huang, H. Chang, *J. Hazard. Mater.* **2017**, *334*, 150–159.
[19] S. Salaeh, D. J. Perisic, M. Biosic, H. Kusic, S. Babic, U. L. Stangar, D. D. Dionysiou, A. L. Bozic, *Chem. Eng. J.* **2016**, *304*, 289–302.
[20] L. N. Chukhlomina, Y. M. Maksimov, L. N. Skvortsova, *Nitride Ceramics: Combustion Synthesis, Properties, and Applications* (Eds.: A. A. Gromov, L. N. Chukhlomina), Wiley-VCH Verlag GmbH & Co. KGaA **2015**, pp. 185–228.
[21] M. N. Solovan, V. V. Brus, E. V. Maistruk, P. D. Maryanchuk, *Inorg. Mater.* **2014**, *50*, 40–45.
[22] O. R. Lourie, C. R. Jones, B. M. Bartlett, P. C. Gibbons, R. S. Ruoff, W. E. Buhro, *Chem. Mater.* **2000**, *12*, 1808–1810.
[23] A. B. Filonov, D. B. Migas, V. L. Shaposhnikov, V. E. Borisenko, W. Henrion, M. Rebien, P. Stauss, H. Lange, G. Behr, *J. Appl. Phys.* **1998**, *83*, 4410–4414.
[24] V. A. Gritsenko, *Phys.-Usp.* **2012**, *55*, 498–507
[25] M. Cheng, G. Zeng, D. Huang, C. Lai, P. Xu, C. Zhang, Y. Liu, *Chem. Eng. J.* **2016**, *284*, 582–598.
[26] P. A. Bhobe, A. Chainani, M. Taguchi, T. Takeuchi, R. Eguchi, M. Matsunami, K. Ishizaka, Y. Takata, M. Oura, Y. Senba, H. Ohashi, Y. Nishino, M. Yabashi, K. Tamasaku, T. Ishikawa, K. Takenaka, H. Takagi, S. Shin, *Phys. Rev. Lett.* **2010**, *104*, 236404.
[27] P. Mytych, P. Cieśla, Z. Stasicka, *Appl. Catal. B* **2005**, *59*, 161–170.
[28] L. N. Skvortsova, L. N. Chukhlomina, T. S. Minakova, M. V. Sherstoboeva, *Rus. J. Appl. Chem.* **2017**, *90*, 1246–1251.
[29] C. Martínez, M. Canle, M. I. Fernández, J. A. Santaballa, J. Faria, *Appl. Catal. B* **2011**, *107*, 110–118.
[30] L. A. Pérez-Estrada, S. Malato, W. Gernjak, A. Agüera, E. M. Thurman, I. Ferrer, A. R. Fernández-Alba, *Environ. Sci. Technol.* **2005**, *39*, 8300–8306.
[31] J. Roscher, M. Vogel, U. Karst, *J. Chromatogr. A* **2016**, *1457*, 59–65.

Submitted: October 23, 2019
Accepted: January 29, 2020